Self-powered and highly efficient ion-diffused $MAPbBr_3$ single crystal-based UV-Vis photodiode

Abida Perveen[1], Yubing Xu[1], Syed Muhammad Abubakar[2], Wei Lei[1]

[1]Joint International Laboratory of Information Display and Visualization, School of Electronic Science and Engineering, Southeast University, Nanjing 210096, China
[2]Beijing National Research Center for Information Science and Technology, School of Integrated Circuits, Tsinghua University, Beijing 100084, China.

***Corresponding Authors**

lw@seu.edu.cn; Tel.: +86 25 83363222; Fax: +86 25 83363222. (L. Wei)

101300071@seu.edu.cn (Abida Perveen)

Abstract:

The p-n junction region of the perovskite single crystals (PSC) made by doping metallic ions through a solution-processed method is too large (more than 10 μm). The carrier drift length (μτE), on the other hand, needs to be greater than the detector's dimension in order to achieve high responsivity. Also, a high bias voltage is required if the p-n junction is particularly thick. For the practical use of a photodiode, a thicker pn junction is not good. So, finding a way to create a narrow p-n junction area of PSC is a need of the time. To achieve this goal, we offer a successful method for generating a narrow p-n junction area by metallic ion diffusion. By narrowing pn junction we have achieved high performance of photodiode with a low trap density (1.6108 cm^{-3}), high mobility (423 $cm^2V^{-1}s^{-1}$), and reduced dark current density (0.5 Acm^{-2}) along with remarkably enhanced responsivity (77.69 AW^{-1}) for 30 Wcm^{-2} UV light at a low applied voltage of 15 V, and detectivity of (1.6 1015 Jones). This method has given a tremendously fast switching speed with a rise/fall duration of 2/6 ns under 0 V bias and long-term stability for more than 3 months in the ambient air. The photodiode performance is studied for UV-Vis light illuminations at various intensities and compared with no diffused photodiode in order to understand the impact of illumination intensity on the narrowed junction-based devices. The results point to a technique that has the potential to create next-level photodiodes.

Secure Quantum Randomness Using Perovskite LEDs

J. Argillander[1], A. Alarcón[1], C. Bao[2,3], C. Kuang[2], G. Lima[4,5], F. Gao[2] & G. B. Xavier[1]

[1] *Department of Electrical Engineering, Linköping University, Sweden*
[2] *Department of Physics, Chemistry and Biology, Linköping University, Sweden*
[3] *National Laboratory of Solid State Microstructures, School of Physics, Nanjing University, China*
[4] *Departamento de Física, Universidad de Concepción, Chile*
[5] *Millennium Institute for Research in Optics, Universidad de Concepción, Chile*

The recent development of perovskite light emitting diodes (PeLEDs) has the potential to revolutionize the fields of optical communication and lighting devices thanks to their simplicity of fabrication and outstanding optical properties [1]. PeLEDs' simplified fabrication process, which eliminates the requirement for cleanroom facilities, holds promise for large-scale quantum technology production at the national level. This could make secure cryptographic solutions widely available, thereby contributing to national security.

Modern quantum random number generators (QRNGs) that certify their privacy are posed to replace classical random number generators in applications such as encryption and gambling, and therefore need to be cheap, fast, and with integration capabilities. Using a compact metal-halide PeLED source we generate random numbers, which are certified to be secure against an eavesdropper, following the quantum measurement-device-independent (MDI) [2] scenario. Our implementation of an MDI-QRNG is able to certify that at least a proportion of 0.71 ± 0.1 of the generated bits are private, i.e. known only to the user of the QRNG and not to an adversary. We run the generator for more than 22 days and record over 8 terabits of data, out of which we randomly sample 5 gigabits that we successfully subject to randomness testing using the NIST 800-22 test suite. The obtained generation rate of more than 10 megabits per second, and an MDI test state success probability of 0.97 ± 0.001, which are already comparable to commercial devices, show that PeLEDs can work as high-quality light sources for quantum information tasks, thus opening up future applications in quantum technologies [3].

Our findings demonstrate the potential of PeLEDs as reliable sources for generating quantum random numbers in secure communication and cryptographic applications. By utilizing the fact that the PeLED can be driven at very low electroluminescence current densities we are able to reach a lifetime of the device of over 22 days of continuous operation, with a projected lifetime of over 45 days of usable bitrate.

References

[1] Chunxiong Bao et al. "Bidirectional optical signal transmission between two identical devices using perovskite diodes". *Nature Electronics* **3** (2020), 156–164. DOI: 10.1038/s41928-020-0382-3.

[2] Jonatan Bohr Brask et al. "Megahertz-Rate Semi-Device-Independent Quantum Random Number Generators Based on Unambiguous State Discrimination". *Physical Review Applied* **7** (2017), 054018. DOI: 10.1103/PhysRevApplied.7.054018.

[3] Joakim Argillander et al. "Quantum random number generation based on a perovskite light emitting diode". *Communications Physics* **6** (2023), 157. DOI: 10.1038/s42005-023-01280-3.

Imaging the invisible – The role of high-performance infrared cameras in environmental sustainability

L. Bendrot[*,1,2], M. Delmas[1], R. Ivanov[1], D. Ramos[1],H. Pettersson[2,3] and L. Höglund[1]

[1] IRnova, Isafjordsgatan 22 C5, SE-16440 Kista, Sweden
[1]Solid State Physics and Nanolund, Lund University, Box 118, 22100 Lund, Sweden
[3]School of Information Technology, Halmstad University, 30118 Halmstad, Sweden

Actions for environmental sustainability are needed at every level in society. Gathering information about temperature and atmospheric gas composition is vital for decision makers, researchers, and industries committed to sustainability and infrared (IR) cameras are the natural choice for this. The IR spectrum covers wavelengths from 700 nm to 1 mm and enables the visualization of heat radiation and gas absorption that remains undetectable in the visible spectrum.

Consider the example of SF_6, an exceptionally potent greenhouse gas that escapes human perception due to its lack of color and odor. The gas plays a vital role in industrial electronic insulation, and each ton of SF_6 leakage is equivalent to emitting more than 20 000 tons of CO_2. It is thus imperative to be able to detect leakages early on. Thanks to IR cameras, this is possible since SF_6 is strongly absorbing at specific wavelengths within the IR spectrum. Another application is heat-mapping of Earth from space with the purpose of providing farmers with information about watering needs over large areas. This is of growing importance as the availability of freshwater becomes scarcer.

A common requirement among IR applications for environmental sustainability is the necessity for high-performance IR cameras. In my research, we are exploring ways to increase IR detector performance in a collaboration between academia and industry. The industry partner IRnova is a Swedish privately owned company with more than 20 years of experience in design and fabrication of IR detectors made from quantum well and type-II superlattice photodetector material. The company's commitment to research and development is poised to pave the way for the next generation of high-performance IR cameras for the acquisition of vital environmental data.

The poster explores the fundamentals of IR detection, delves into IR sustainability applications, and highlights ongoing research within IR detector performance at IRnova.

*Corresp. author: linnea.bendrot@ir-nova.se, Phone: +46-734-038-356

Fabrication of a Flexible X-Ray Detector using Silica Capillary Fibres Filled with Scintillating Liquid

Magnus Lindblom[1], Maximilian Patzauer[1], Nazila Safari Yazd[1], Ulrich Vogt[3], Scott Wilbur[2], Walter Margulis[1], Joao Pereira[1], Kenny Hey Tow[1], Åsa Claesson[1], Timothy Gibbon[1], Sven-Christian Ebenhag[1]

1. *Research Institutes of Sweden, Isafjordsgatan 22,164 40 Kista, Sweden*
2. *University of Sheffield, Western Bank Sheffield, S10 2TN, United Kingdom*
3. *Royal Institute of Technology, Roslagstullsbacken 21, 114 21 Stockholm, Sweden*

We present a fabrication process and measurement results of scintillating fibre components for X-ray detection based on liquid filled silica capillaries. The development is part of the FleX-RAY project [1], which aims to create a digital X-ray detector for imaging of curved surfaces that is both flexible and capable of self-reporting its shape (see Fig 1a). A web of scintillating optical fibres will detect the X-rays and guide the scintillation light to silicon photomultipliers. Both liquid-filled silica capillaries and plastic scintillating fibres (PSF) can be used in the detector, as suggested already in 1960 [2]. It has been shown that the liquid filled fibres have potentially higher resistance to radiation damage than PSF [3]. In addition, the liquid filled fibres provide flexibility in the choice of scintillator since they can be filled with different types of scintillating cocktails, i.e., high-Z loaded liquids for enhanced X-ray attenuation. The hole diameter can be chosen to match the spatial resolution requirement of the application.

Here, we present both performance results and details of the fabrication methodology. Comparative measurements were performed, between a PSF (SCSF-78, Kuraray) and silica optical fibre components. The optical fibre components are based on capillaries filled with a liquid scintillator (BC505, Saint-Gobain), see Fig.1b. The scintillation spectrum was measured at one end of the fibres during exposure to X-rays (Excillum MetalJet D2 source, 24-keV line emission and 70 kV acceleration voltage). The result indicates three times more scintillation light at the detector per cross-sectional area for the liquid filled fibre compared to the PSF.

Fabrication steps include filling capillary fibres with liquid scintillator and splicing of speciality fibres. Multimode fibres are used to guide light signals produced during scintillation to detectors. The capillary components, see Fig. 1c, are based on a central capillary, typically 20 cm long, with a 50 µm inner diameter with a 20-cm piece of 8-µm capillaries is spliced to each end. The component is filled with scintillating liquid and capped by splicing solid silica fibres to the capillaries. The entire component is coated with a low index cladding (OF-133-V3, myPolymer) to improve the optical trapping efficiency. The 8-µm capillaries act to reduce optical losses caused by the liquid to air interface in the capillary.

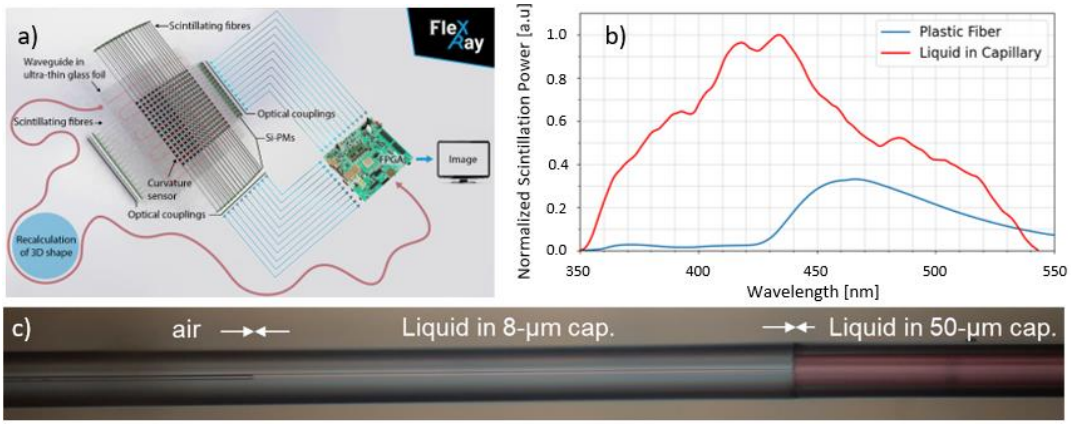

Fig. 1. a) A concept overview of the fiber-based, flexible, shape self-reporting X-ray detector. b) Comparison of the low-pass filtered scintillation spectrum from an liquid filled fibre component and a plastic scintillating fibre (PSF). c) A microscope image of a fibre component, filled with a red dye for visibility. The liquid-air interface causes optical losses and is preferably located in a small-diameter capillary.

References

[1] S. Wilbur, *et al*., "Flexible X-ray imaging detectors using scintillating fibres," JINST 17, C10013 (2022)
[2] L.Reiffel, *et al*., "Some Considerations on Luminescent Fiber Chambers and Intensifier Screens," Rev. Sci. Instrum., 31, 1136 (1960)
[3] S.V Golovkin, *et al*., "Radiation damage studies on new liquid scintillators and liquid-core scintillating fibers," Nucl. Instrum. Meth. Phys. Res. A, 362, 283 (1995).

Optical properties of Au/Ge/HfO_2 stack of thin films for possible applications in waveguides with absorbing sidewalls

Varis Karitans, Martins Zubkins
Institute of Solid State Physics, University of Latvia

Thin absorbing films are widely studied due to their wide range of applications [1]. One possible application is their use as absorbing refractive waveguides arranged in a stack and forming diffraction patterns of the vectors of a two-dimensional input object. Such diffraction patterns may be used to accelerate the phase retrieval of two-dimensional objects.

In this study, we are investigating the reflectance maps of Au/Ge/HfO2 stack of thin films depending on the incident angle and wavelength, and the state of polarization. Au/Ge thin films are known as very good absorbers in a wide range of wavelength and the angle of incidence for two orthogonal polarizations. HfO_2 is selected due to its high refractive index and low chromatic dispersion. The stack of thin films is fabricated using the thermal evaporator and R&D multifunctional vacuum coater SAF25/50. The thicknesses of Au/Ge/ HfO_2 thin films are 51 nm/15 nm/1000 nm, respectively. The stack was formed on a silicon wafer. The reflectance maps of the stack were measured for both s- and p- polarization using a spectrophotometer Cary 7000. The reflectance was measured in the spectral range of between 400 nm and 700 nm at the incident angles covering the range from 10 to 80 degrees.

Figure 1 shows the reflectance maps of the stack of the thin films. The angle of incidence varies along the x-axis, while the wavelength varies along the x-axis. The reflectance is given in percent. The top and bottom panel show the data for s- and p-polarized light, respectively.

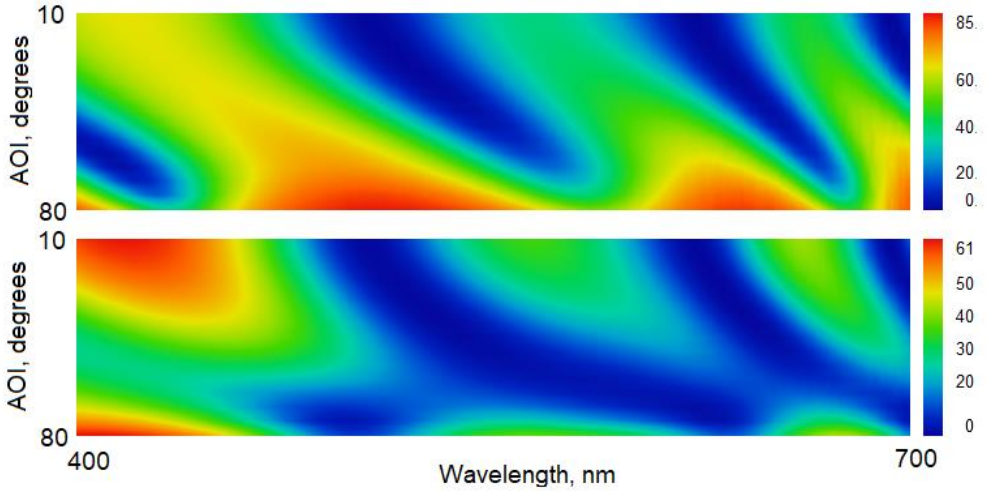

Figure 1. The dependence of reflectance (%) on the wavelength and the angle of incidence (AOI). Top panel: s-polarization, bottom panel: p-polarization

There are wavelengths at which there is very low reflectance across the whole range of AOI. This would allow to separate individual vectors which could be processed in parallel by high-speed processors thus enabling phase retrieval in real-time.

1. M. ElKabbash, S. Iram, T. Letsou, M. Hinczewski, G. Strangi. Designer perfect light absorption using ultrathin lossless dielectrics on absorptive substrates. Advanced Optical Materials 6(22), 1800672, 2018.

The study is supported by the University of Latvia Foundation and the company MikroTik (project # 2257).

Self-compression of NIR pulses in single-domain KTP

Christoffer Krook[1], Anne-Lise Viotti[1,2], Björn Hessmo[1], Fredrik Laurell[1], Valdas Pasiskevicius[1]
1: Royal Institute of Technology KTH, Roslagstullsbacken 21, 10691 Stockholm, Sweden
2: Department of Physics, Lund University, P.O Box 118, SE-221 00 Lund, Sweden

Ultrashort femtosecond pulses are today employed in various areas including industrial-, medical- and fundamental science applications. In recent years, solid state sources such as Yb-based systems have gained popularity due to excellent beam quality and efficient heat dissipation. The gain-bandwidth of Yb however limits pulse durations to 100s of femtoseconds [1]. For this reason, pulse post compression is required to reduce the temporal duration further. Popular methods include multi-pass cells and nonlinear spectral broadening in fibers followed by conventional compressors [1, 2]. The complexity and size of such implementations however motivates research into alternative compression methods. Here we demonstrate a new and novel pulse compression technique, relying on the utilization of Raman modes and polaritons in KTP to achieve self-compression in the normal dispersion regime.

KTP has a rich optical phonon spectrum which can couple strongly to laser radiation by the formation of phonon-polariton waves [3]. The dispersion of the polariton waves allows for intra-pulse difference-frequency generation of polaritons. The polaritons will then in turn generate sidebands through modulation with the laser pump pulse through the electro-optic effect [4]. As a pump-pulse propagates through KTP, sidebands are initially generated on the tail of the pulse. As the pump then travels through the material, material dispersion enables these sidebands to temporally catch up with the pump pulse. When this happens, cascaded generation of Stokes-sidebands occur, and pulse compression as a result of this.

The experimental setup consists of a commercial Yb fiber laser providing 170-fs pulses with an average power of up to 20 mW and a 21.2 kHz repetition rate. This pulse is focused with a 150-mm lens after which it is incident on a 12x8x5 mm bulk KTP crystal. The laser radiation is polarized along the crystal z-axis and is propagating along the x-axis. The focus spot size has a 21 µm $1/e^2$-radius, and the crystal position with respect to the focus position was controlled with a motorized translation stage. After propagation through the crystal, the beam is collimated and passed into an X-FROG device for temporal full-field characterization and an optical spectrum analyzer.

With this method we achieved pulse durations of 19.5 fs, showing a compression factor greater than 9. The beam profile after propagation remains gaussian and the resulting spectrum stretches from 0.95 µm to 1.45 µm. Both temporal and spectral intensity can be seen in fig. 1 a) and b).

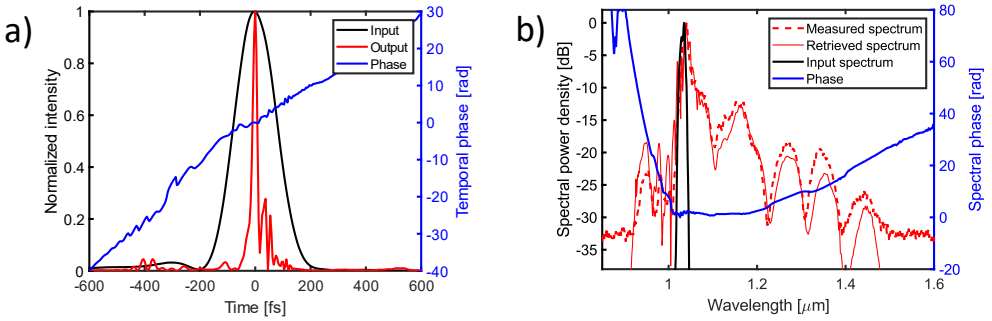

Figure 1. a) Temporal intensity of pump (black) pulse and compressed (red) pulse together with phase of compressed pulse (blue). b) Pump-spectrum (black) together with compressed pulse spectrum (red) and spectral phase of the compressed pulse (blue).

In conclusion we have here demonstrated self-compression of NIR femtosecond pulses in the normal dispersion regime in KTP. The concept does not rely on solitons and thus power-scaling should be possible.

[1] Seidel, M., Brons, J., Arisholm, G. *et al.* "Efficient High-Power Ultrashort Pulse Compression in Self-Defocusing Bulk Media," Sci Rep 7, 1410 (2017).
[2] Coluccelli, N., Viola, D., *et al*. "Tunable 30 fs light pulses at 1W power level from a Yb-pumped optical parametric oscillator", Opt. Lett. 42, 4545-4548 (2017).
[3] Pasiskevicius, V., Canalias, C., Laurell, F., "Highly efficient stimulated Raman scattering of picosecond pulses in KTiOPO4 ", Appl. Phys. Lett. 88, 041110 (2006).

[4] Shen, Y., Watanabe, T., *et al*. “Nonlinear Cross-Phase Modulation with Intense Single-Cycle Terahertz Pulses”, Phys. Rev. Lett, 99, 043901 (2007).

Titel:
Latest Generation Ultrafast Lasers For Non-Linear Microscopy: Towards Seamless Integration

Abstract:
Multiphoton microscopy enjoys applications and variations continuously emerging in diverse branches of neuroscience, cancer studies, and stem cell research. The push to employ the advantages of multiphoton imaging for clinical and diagnostic applications is gaining momentum both on the research and commercial front. An increasing number of fluorescent probes as well as new laser beam manipulation, optical delivery, and excitation schemes are introducing innovative approaches. Commercial microscope companies are offering more advanced set ups where increased laser power, dispersion pre-compensation or modulation techniques are required to achieve imaging with wider field of view, faster acquisition rates or imaging deeper into a tissue. These advancements are a strong driving force for the continuous improvements in parameters and functionality of the commercial femtosecond laser sources, which are fundamental in driving the nonlinear excitation process.

Författare:
Darryl McCoy, Mantas Butkus, Marco Arrigoni

Finns det plats för oss?

Med vänliga hälsningar,

Mikael

Mikael Winters, PhD
Area Sales Manager, Scientific Research & Instrumentation
Coherent
Aminogatan 30
SE-431 53 Mölndal, Sweden
Office : +46 31 10 22 18
Mobile : +46 795 852 239 (Sweden)
mikael.winters@coherent.com
www.coherent.com

The first backward wave optical parametric oscillator waveguide

Patrick Mutter, Fredrik Laurell, Valdas Pasiskevicius and Andrius Zukauskas
Department of Applied Physics, Royal Institute of Technology, Roslagstullbacken 21, 10691, Stockholm, Sweden

Backward wave optical parametric oscillators (BWOPO) [1] represent a paradigm shift in optical parametric oscillation. In a conventional optical parametric oscillator, the generated signal and idler propagate forward in the direction of the pump. In contrast, a BWOPO generates signal and idler that counter-propagate. The anti-parallel nature of the nonlinear interactions allows for distributed feedback without needing a cavity, making the BWOPO a robust, easy to align and highly efficient single-pass device.

Since one downconverted photon counter-propagates the pump, the momentum mismatch of the interaction is enormous. Hence quasi-phase-matching (QPM) with sub-µm periodicities in $KTiOPO_4$ (KTP) provides today the only viable route for realizing a BWOPO. It was previously demonstrated that the fabrication challenges can be overcome by coercive field engineering [2], allowing consistent fabrication of sub-µm domain gratings in bulk KTP. However, the delicate nature of these finely-pitched domain structures makes them vulnerable to heat treatment that is necessary for ion-exchanged waveguides in KTP [3], which has prevented a BWOPO implementation in a waveguide so far. In this work, we demonstrate how these fabrication challenges can be surmounted by utilizing segmented waveguides.

In this approach, an ion exchange grating is first inscribed into KTP that serves as the waveguide and the coercive field grating simultaneously. Subsequently, the waveguide is periodically poled, eliminating the need for any subsequent heat treatment. Fig. 1 (a) shows a PFM image of such a waveguide with a QPM period of 409 nm. To evaluate the optical performance of the waveguides, 215 ps long pulses of a Ti:Sapphire regenerative amplifier were coupled into the waveguide. Fig. 2 (b) presents the conversion efficiency and the output energy of the parametric waves as a function of the pump energy. The threshold for oscillation is at a pump energy of 325 nJ, representing a remarkable 19-fold reduction compared to a recent bulk BWOPO experiment pumped with the same laser [4]. Transmission measurements below the threshold reveal 92% transmission over 22 mm length (0.16 dB/cm) underscoring the waveguide's low loss characteristics. Other important features of the BWOPO waveguide will also be discussed.

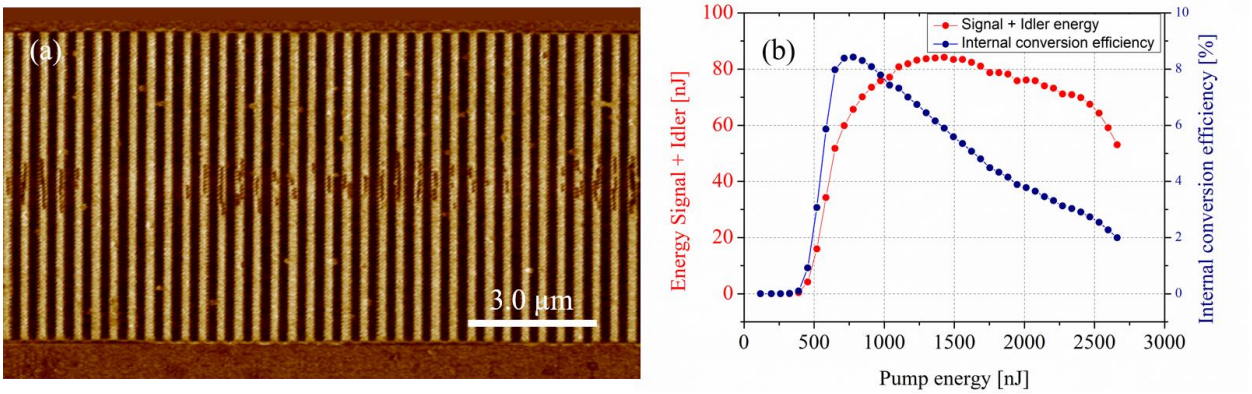

Fig. 1 (a) PFM images of segmented and periodically poled waveguide. (b) Conversion efficiency and output energies as a function of pump energy

References

1. C. Canalias and V. Pasiskevicius, "Mirrorless optical parametric oscillator," Nat. Phot. **1**, 459–462 (2007).
2. P. Mutter, A. Zukauskas, and C. Canalias, "Domain dynamics in coercive-field engineered sub-µm periodically poled Rb-doped $KTiOPO_4$," Opt. Mater. Express **12**, 4332–4340 (2022).
3. P. Mutter, C. C. Kores, F. Laurell, and C. Canalias, "Ion-exchanged waveguides in periodically poled Rb-doped KTiOPO4 for efficient second harmonic generation," Opt. Express **28**, 38822–38830 (2020).
4. P. Mutter, A. Zukauskas, A. L. Viotti, C. Canalias, and V. Pasiskevicius, "Phase-locked degenerate backward wave optical parametric oscillator," APL Photonics **8**, (2023).

ACCURATE MEASUREMENT OF DRIVERS' REACTION TIMES IN THREE DIFFERENT ROAD LIGHTING SETTINGS

Nilsson Tengelin, M[1], Källberg, S.[1], Lindgren, M.[1], Ebenhag, S-C.[1]
[1] Department of Measurement Science and Technology, RISE Research Institutes of Sweden, Borås, SWEDEN
Maria.Nilssontengelin@ri.se

Abstract

This poster presents a study on the measurements the reaction time of a car drivers and how this reaction time is influenced by the road lighting. Three different road lighting settings (two with constant output but different light levels and one modulated) were tested in the city area of the car test track AstaZero. Suddenly appearing targets placed along the track were used to trigger a response to brake. The reaction time was measured by time stamped recordings of the target movement and brake pedal pressure. Release of the gas pedal was also recorded, and time stamped. 40 research persons drove 12 laps each, one driver at the time, where the lighting setting and which target would appear was altered between each lap. Each road lighting setting was selected four times in a randomized order. Preliminary analysis of the reaction time data indicates no influence of the modulated lighting on the reaction time but a slight tendency that the reaction times are increased with a lower light level.

Keywords: Reaction Time, Temporal light modulation, Road lighting, Driver

Figure 1 – The test track on Asta zero. Setting up the test road (left) and trial run (right).

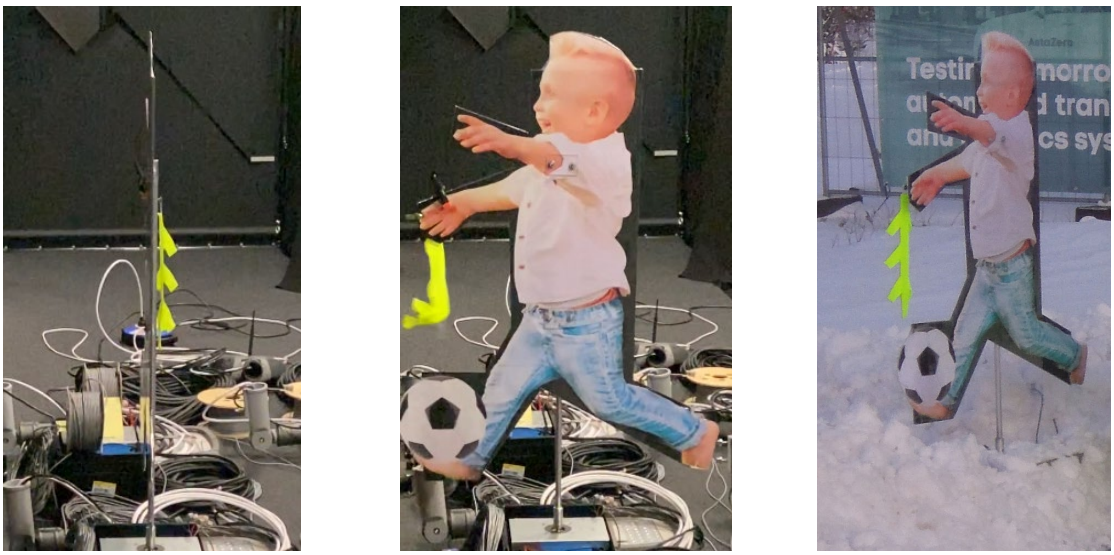

Figure 2 – Reaction target during testing in the lab (left) and on the test track (right).

Sensor Integration: Exploring the Potential of Fiber Bragg Gratings in High-Temperature 3D Printed Components

M. Patzauer[1], C. Sterner[1], B. Verma[2], M. Mürer[3], Saeed Khademzadeh[4]

[1]*RISE Research Institutes of Sweden, Fiber Optics and Photonics, Isafjordsgatan 22, 164 40, Kista, Sweden*
[2]*Chair of Digital Additive Production (DAP), RWTH Aachen University, Aachen, Campus Boulevard 73 52074, Germany;*
[3]*LINDE GMBH, Dr.-Carl-von-Linde-Str. 6-14, Pullach, 82049, Germany;*
[4]*RISE IVF AB, Argongatan 30, Mölndal, 431 53, Sweden;*

Corresponding author: maximilian.patzauer@ri.se

This ongoing study explores how to integrate Fiber Bragg Grating (FBG) sensors into components produced using high-temperature 3D printing, specifically, laser-based powder bed fusion for metals (PBF-LB/M). FBG sensors, known for their ability to measure temperature and strain with precision, offer versatile solutions for real-time monitoring in various applications.

To demonstrate the practicality of FBGs we design channels in an additively manufactured gas burner head, considering factors like bending radius and powder removability. We address the challenges encountered during post-processing and investigate feasible solutions to ensure seamless FBG integration after the PBF-LB/M process.

In our testing, we expose the FBG sensors to temperatures reaching 1000°C. We take care to calibrate the sensors accurately and monitor for any drift, particularly at 800°C. This research contributes insights to the advancement of sensor integration techniques in additive manufacturing.

Keywords: FBG Sensor; Sensor integration; Component design; Additive Manufacturing; Laser Powder Bed Fusion

OPD : Poster abstract Submission

Novel Sub 50 fs for improved multiphoton microscopy

Abstract

An increasingly large number of published results in various biomedical fields rely on multiphoton excitation and microscopy, for high-resolution three-dimensional live-cell imaging, where single photon techniques are limited by out-of-focus fluorescent background and penetration depth. Looking deep inside complex biological specimens highlights the many advantageous effects resulting from a localized multiphoton illumination. The efficiency in multiphoton excitation is strongly dependent on the peak power of the incident light during the pulse. As such, the shorter the pulse, the higher the peak power and the stronger the generated multiphoton signal. In live cell microscopy, photodamage is one of the main limiting factors when observing living cells or tissue over extended periods of time. While phototoxicity is also function of molecular structure and the experimental environment, it is inevitably accelerated by constant exposure to a high average laser power (Table 1 shows the comparison of average power needed for 200 fs and 50 fs pulses).

Ultrafast laser technologies, delivering ultrashort femtosecond pulses with high peak powers, increase the likelihood of simultaneous multiphoton events, but up till now there has been relatively limited ability to generate ultrashort pulses below the 80 fs limit. In this presentation, we discuss the advantages of sub 50 fs pulses (typically 35 - 40 fs) and show examples of how these ultrashort pulses result in higher multiphoton efficiency due in principle to the higher peak power and hence drastically improves signal brightness (Figure 1 shows how the signal brightness changes with pulse durations). For live-cell imaging, sensitive to phototoxicity, the combined lower average laser power and high peak power delivered by sub 50 fs pulses enhance cell viability and considerably extend imaging.

Pulse Duration	**Peak power** (30 MHz)	**Average Power** *For the same TPEF
200 fs	16 kW	100 mW
50 fs	16 kW	25 mW

Table 1: Pulse duration, peak power and average power comparison

Figure 1: Third harmonics of a calibration grid (Ibidi) with 50 micrometer squares. a) 4.7 mW, full spectrum short pulses (<50 fs). b) 6 mW with laser spectrum limited to 10 nm bandwidth (~160 fs). c) Scaled up contrast for the 6 mW laser spectrum limited to 10 nm bandwidth (~160 fs).

.

Authors: Oliver Prochnow, Dirk Mortag, Jan Ahrens. VALO Innovations GmbH – A part of Hübner Photonics, Hollerithallee 17 30419 Hannover Germany.

Acknowledgment: The authors wish to thank Dr. Marloes Groot, Professor, Biophotonics and Medical Imaging, Faculty of Science, LaserLab, Vrije Universiteit Amsterdam, The Netherlands, for help with the experiments.

Optical concentration effect in fully delineated mid-wave infrared T2SL SWaP HD detectors arrays.

D. Ramos[*,1,2], M. Delmas[1], L. Höglund[1], R. Ivanov[1], L. Žurauskaitė[1], D. Evans[1], D. Rihtnesberg[1], L. Bendrot[1] S. Smuk[1], A. Smuk[1], S. Becanovic[1], S. Almqvist[1], P. Tinghag$_1$, S. Fattala[1], E. Trybom[1] and E. Costard[1]

[1] IRnova AB Electrum 22 - C5, SE-164 40 Kista, Sweden
[2] School of Electrical Engineering and Computer Science KTH Royal Institute of Technology, SE-164 40 Kista, Sweden

Type-2 Superlattices (T2SL) offer numerous advantages over classical midwave infrared (MWIR, 3-5 μm) detectors. Operating temperatures up to 150 K have been recently demonstrated in VGA format (640 × 512 pixels, 15 μm pitch) T2SL focal plane arrays (FPAs). The resulting lower cooling requirement enables detector packaging with reduced size, weight, and power consumption (SWaP).

Next step is to produce high operating temperature (HOT) HD arrays (> 1280 × 1024 pixels) with small pixel sizes (< 10 μm). However, further reduction of the pitch size is a challenge for the system, as very small areas need to be defined in the semiconductor. Unlike planar technologies, T2SL pixels are typically defined by etching trenches in the semiconductor. This procedure may compromise the operating temperature of the detector by degrading its electrical and optical performance. In the former aspect, exposing the pixel sidewalls can increase the dark current with a surface leakage component. In the latter, reducing the optically sensitive area impacts both quantum efficiency (QE) of individual pixels and the modulation transfer function (MTF) of their array.

In this study, the relationship between quantum efficiency (QE) and pixel size is studied theoretically and experimentally in fully delineated MWIR T2SL detectors. Measurement on the arrays with different pixel sizes (down to 10 μm) demonstrate no impact of the reduced size on the dark current density and positive impact – on the QE. Using 2D simulations in COMSOL, we explain the latter effect as improved absorption efficiency in the detector structure due to light diffraction on the trenches. We also analyze the impact of this diffraction on the array performance by measuring the MTF in a set of FPAs with varying width and depth of trenches.

*Corresp. Author: david.ramos@ir-nova.se, Phone: +46 879 366 23

Figures

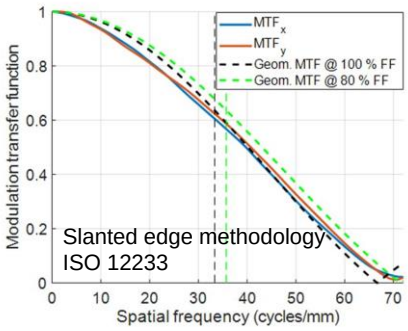

Fig. 1. MTF calculated from the edge spread function in x- and y- directions compared to the ideal values for an ideal 15 um pitch detector.

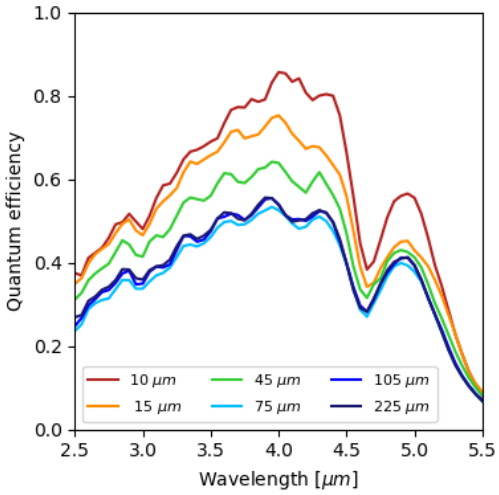

Fig. 2. QE measured at 140 K for the different pixel sizes.

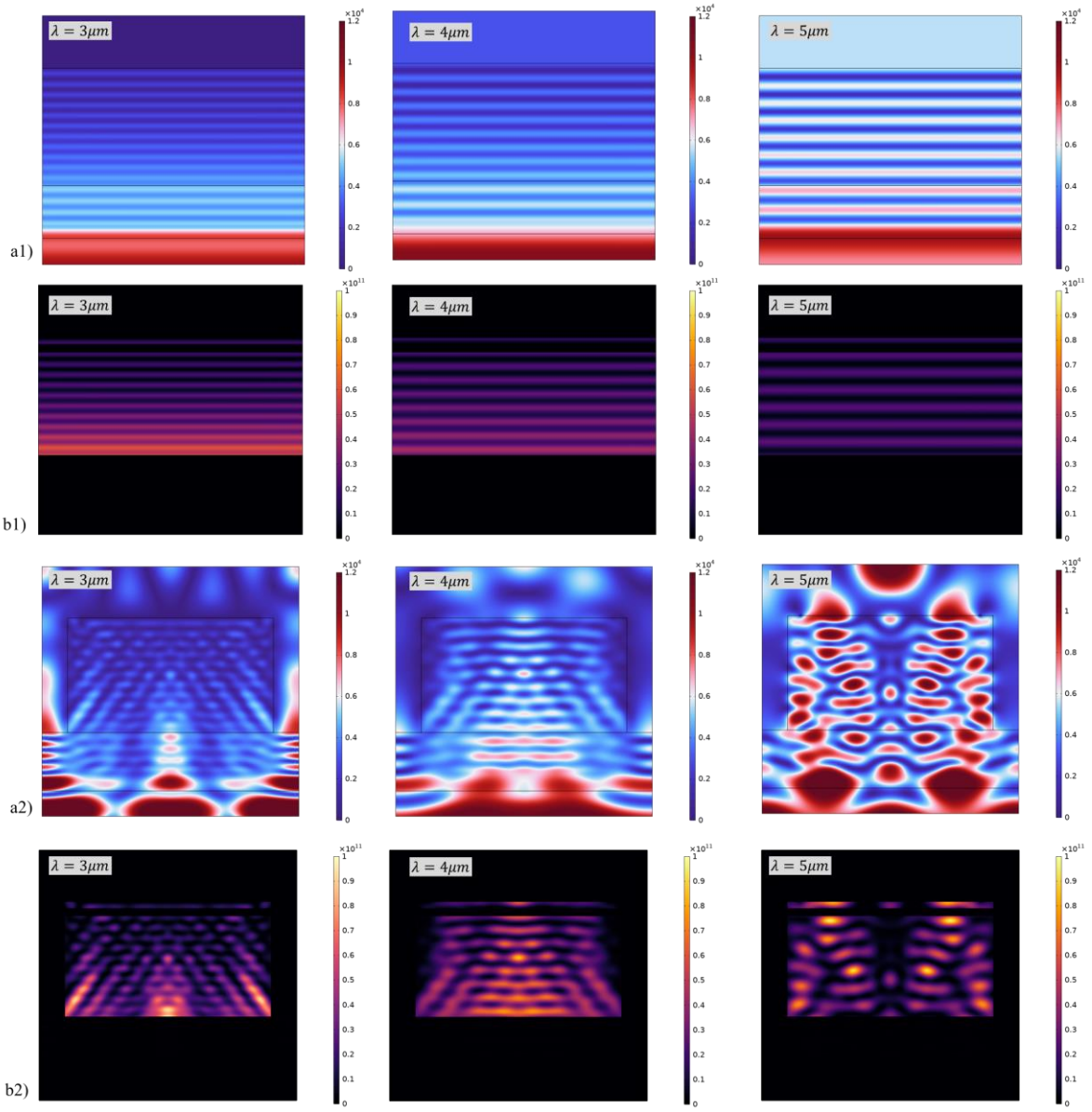

Fig. 3. 2D simulation of (a) the normalized electric field distribution (V/m) and (b) absorption distribution (W/m)

a1, b1) 10 µm of non-delineated material (FF=1).

a2, b2) delineated material with an 8 µm pixel on a 10 µm pitch.

Design and fabrication of silicon-integrated high-frequency telecom-wavelength photonic-crystal surface-emitting lasers

Olof Sjödin, Axel Strömberg, Ishwor Koirala and Mattias Hammar

Department of Electrical Engineering, Royal Institute of Technology, Electrum 229, 164 40 Kista, Sweden

Corresponding author: olsj@KTH.se

Photonic-crystal surface-emitting lasers (PCSELs) have the potential for large-area singlemode emission by virtue of Bragg reflection from a two-dimensional standing-wave mode confined by a buried photonic crystal (PC) layer in close proximity to an activated gain region [1]. Such ultra-compact singlemode high-power laser devices with narrow-beam divergence have ample of potential applications in materials processing, optical communication and sensing. Near-infrared GaAs-based PCSELs with watt-range continuous-wave output power have been demonstrated [2], but there are no similar results reported for their longer-wavelength counterparts in the InP-based materials system. Furthermore, while all PCSELs fabricated to date have been large-area discrete devices designed for high-power emission, there would be important applications in optical fiber communication for lower-power singlemode devices with improved high-frequency modulation, especially if they can be mass-produced in a parallel fashion using planar technologies. Here we report on the development of 1.55-μm hybrid InP/Si PCSELs by direct integration on silicon wafer using micro-transfer-print technology [3,4].

[1] S. Noda, K. Kitamura, T. Okino, D. Yasuda, Y. Tanaka, IEEE J. Sel. Top. Quantum Electronics 23, 1 (2017)
[2] Y. L. Hirose, Y. Kurosaka, A. Watanabe, T. Sugiyama, S. Noda,Nat. Photonics 8, 406 (2014)
[3] D. Zhao, S.-C. Liu, H. Yang, Z. Ma, C. Reuterskiöld Hedlund, M. Hammar, W. Zhou, Scientific Reports 6, 18860 (2016)
[4] C.R. Hedlund, S.C. Liu, D. Zhao, W. Zhou, M Hammar, Physica Status Solidi, 217 (3), 1900527 (2020)

Laser-induced Graphene Electrodes for Flexible Solar Cells

Vivek Kumar, Sudhansu Sekhar Nath, and Poonam Sundriyal

Printing and Flexible Device Manufacturing Laboratory, Department of Mechanical Engineering, Indian Institute of Technology, Kharagpur, India, 721302

Corresponding author: psundriyal@mech.iitkgp.ac.in

Abstract

Flexible, lightweight, and mechanically robust solar cells are urgently required to power next-generation smart electronics such as touch panels, wearable sensors, light-emitting diodes, etc. Graphene is an attractive material for photovoltaic solar cells due to its high mobility, good transparency, long-term stability, and other electronic and optical properties. However, the traditional and complex processing of graphene reduces its electrical and optical performance. Here, we report a one-step fabrication of high-quality graphene electrodes from polyimide sheets using a 10.6 μm CO_2 Laser. The formation of highly conductive Laser-induced graphene (LIG) with few layers of graphene was confirmed by Raman analysis and four-probe electrical measurements. The crystallinity and morphology of the LIGs were checked by X-ray diffraction spectroscopy (XRD) and scanning electron microscopy (SEM). The developed LIG was used as a flexible counter electrode for the solar cell. The perovskite layer was formed by depositing PbI_2 and CH_3NH_3I aqueous mixture and its sintering by laser irradiation. The [6,6]- phenyl-C61-butyric acid methyl ester was further printed on the perovskite layer, and silver electrode was deposited at the top to complete the perovskite solar cell device. The fabricated solar cell device exhibited a power conversion efficiency of ~ 14 %. It also demonstrated excellent flexibility with no change in device performance under bending upto 140º. Further, this device was integrated with a flexible LIG-NiO supercapacitor to develop a self-powered device. The present work demonstrates high potential of Laser for improved fabrication of solar cells and its potential for improved manufacturing of smart electronics.

High-resolution high-speed µ-LIBS microscope

A.Tercier[1,2], E. Vasileva[3*], C. Alvarez-Llamas[1], C. Fabre[4], S. Hermelin[1], F. Trichard[2], C. Dujardin[1], V. Motto-Ros[1,2**]

Corresponding authors: * elena.vasileva@hubner-photonics.com, ** vincent.motto-ros@univ-lyon1.fr

[1] Institut Lumière Matière UMR 5306, Université Lyon 1 – CNRS, Université de Lyon, 69622 Villeurbanne, France.

[2] Ablatom S.A.S., Villeurbanne, France.

[3] Cobolt AB, a part of Hübner Photonics

[4] GeoRessources, UMR CNRS 7366, Université de Lorraine, F-54500 Vandoeuvre-les-Nancy, France

[5] Optoprim, Vanves, France

Laser-Induced Breakdown Spectroscopy (LIBS) is gaining increasing popularity as an analytical method for determining material composition due to its exceptional sensitivity and its ability to detect elements from the entire periodic table with minimal constraints on sample size, consistency, or surface quality. The recent introduction of LIBS imaging has expanded the capabilities of this technique even further. LIBS imaging allows for the creation of maps displaying the distribution of elements or minerals within an analysed sample.

Traditionally, LIBS analysis has utilized excitation sources, like lasers, with a repetition rate ranging from 10 to 100 Hz, offering a reasonable balance between sampling frequency and laser pulse energy. However, to efficiently produce high-resolution µm-scale LIBS images of large sample areas (several cm^2), a higher repetition rate is necessary to prevent excessively long acquisition times.

This study presents an approach aimed at reducing the acquisition time for high-resolution µ-LIBS imaging by employing a laser operating in the kHz frequency range. The increased laser repetition rate has facilitated the development of a µ-LIBS imaging microscope capable of generating images with approximately 10 µm resolution within less than 20 minutes per cm^2. For the first time, this method has made it possible to create images with nearly 4K resolution, revealing detailed elemental distribution within an analysed sample. This system's ability to rapidly perform LIBS analysis over extensive samples and elucidate the spatial distribution of elements within the analysed region opens opportunities for a wide range of research fields, including biomedical and geological material analysis, as well as applications in industrial settings such as mining.

Acknowledgement

This work was partially supported by the French region Rhônes Alpes Auvergne (Optolyse, CPER2016), the French "Agence Nationale de la Recherche" (ANR-22-xxx "MEMOar" and ANR-20-CE17-0021 "dIAg-EM), and the French government "Plan de Relance" and "France 2030" (ANR-22-PEXD-0014, "Libelul") under the DIADEM program managed by the "Agence Nationale de la Recherche" (ANR-22-PEXD-0014, "Libelul"). In addition, we gratefully acknowledge Jean Michel Laurent, Shayne Harrel, Antoine Varagnat from Andor Technologies.

Lifetime measurements of Er/Al co-doped gain fibers

Tim Wörmann, Martin Brunzell, Pawel Maniewski, Fredrik Laurell, Valdas Pasiskevicius

Department of Applied Physics, Royal Institute of Technology, Roslagstullbacken 21, 106 91 Stockholm, Sweden

Many fields have benefitted from the use of fiber amplifiers such as long-distance communications [1], medical imaging [2], spectroscopy [3] and sensing for example for military purposes [4]. However, there are limits of modern fabrication techniques, such as modified chemical vapor deposition (MCVD), of such fibers due to an effect called concentration quenching. This undesired effect limits the possible doping concentrations by ion interactions in the medium, effectively quenching the radiative ions in question. A way to probe the concentration quenching and gaining a deeper understanding of where it arises can be done by carefully examining the lifetime of the radiative medium in the fiber. In this work we present a method of measuring lifetimes of Erbium 3+ (Er3+) doped fibers and a study into the effect of heat induced quenching is also presented.

For many applications high lifetimes are desired and the end goal is to fabricate fibers with both high doping concentration and lifetimes. A challenge with fabrication is quenching effects that arise when doped fibers are concentrated highly. When two nearby pairs of ions get excited, a fast energy transfer can happen from one ion to the other, which is more probable in high doping concentrations. This new state decays rapidly leading to a waste of energy which constitutes to a negative effect in amplifier performance. This clustering also happens when exposing the heat and causing rearrangements of Erbium ions. To study this an in-house single-mode Er/Al co-doped gain fiber is fabricated and subject to rigorous lifetime measurements. The idea is to pump the Erbium doped fiber (EDF) at λ_p = 976 nm and stimulate the fluorescence around λ_s = 1530 nm. The perpendicular two-beam setup is shown in Fig.1. where a CO2 laser is used as a heat source and the 976nm pump together with a fast avalanche photodiode probes the lifetime.

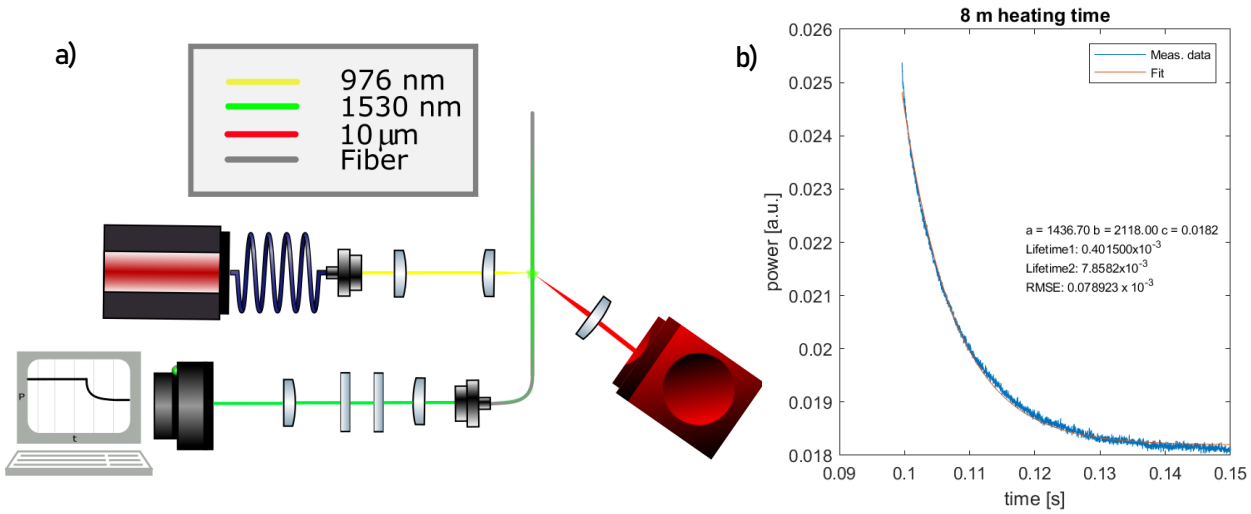

Fig. 1: a) Schematic of the setup. b) Measured lifetime with a double exponential fit, yielding a lifetime of 7.858 ms for 8 min of heating.

References

[1] Li, T. (1993). The impact of optical amplifiers on long-distance lightwave telecommunications. Proceedings of the IEEE, 81(11), 1568-1579. doi: 10.1109/5.247728.

[2] Tang, Y., et al. (2008). A powerful new tool for medical imaging and industrial measurement. SPIE Newsroom.

[3] Webber, M. E., Pushkarsky, M., & Patel, C. K. N. (2003). Fiber-amplifier-enhanced photoacoustic spectroscopy with near-infrared tunable diode lasers. Applied optics, 42(12), 2119-2126. doi: 10.1364/AO.42.002119.

[4] Kyselak, M., Vavra, J., Slavicek, K., Grenar, D., & Hudcova, L. (2023). Long Distance Military Fiber-Optic Polarization Sensor Improved by an Optical Amplifier. Electronics, 12, 1740. doi: 10.3390/electronics12071740.

Metasurface Thermal Emitter for Gas Sensing Application

Prince Gupta, Shaomin Li, Yuanrong Zhang, Max Yan*

Department of Applied Physics, KTH Royal Institute of Technology, Sweden
*maxyan@kth.se

Abstract: A narrow-band, on-chip MIR source (4.3μm) for gas sensing based on MEMS heater and metal-insulator-metal metasurface structure is developed successfully. Both electro-thermal and electromagnetic performances of the emitter are designed and optimized with COMSOL Multiphysics. The integrated MIR source is fabricated in AlbaNova Nanolab, and is characterized using IR camera, thermocouple, and FTIR spectrometer.

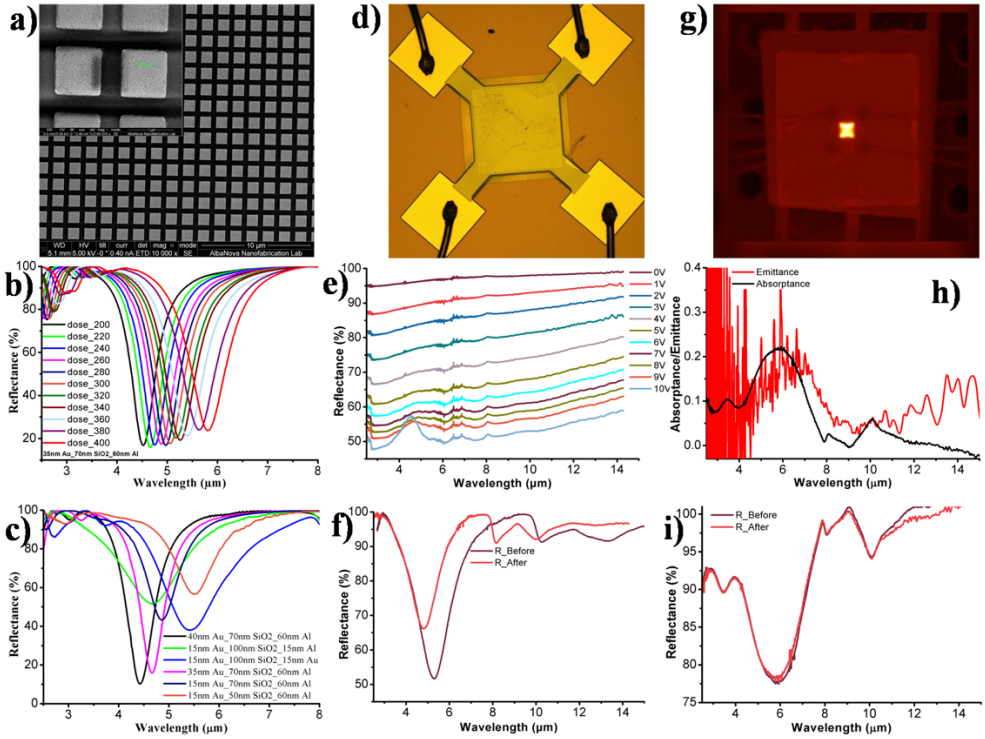

Figure 1. (a) SEM image of three-layer metasurface emitter. (b) Measured reflectance of fabricated metasurface with different top Au particle width. (c) Reflectance spectra of metasurface structure with various combination of layer thicknesses. (d) Microscope image of integrated metasurface emitter. (e) Measured normalized reflectance at various heater temperature using FTIR microscope. (f) Reflectance of a selected metasurface emitter before and after heating experiment. (g) IR camera image of a heater. (h) Measured emittance at 220°C of a metasurface emitter. (f) Reflectance of an emitter before and after emission experiment.